MDPI

Article

Balancing Economic Growth, Carbon Emissions, and Sequestration: A Multi-Objective Spatial Optimization in Zhengzhou Metropolitan Area in China

Mengze Fu, Kangjia Ban, Li Jin and Di Wu *

School of Architecture, Zhengzhou University, Zhengzhou 450001, China; ffpikaq@zzu.edu.cn (M.F.);
bkj230778@163.com (K.B.); jinliurban@163.com (L.J.)
* Correspondence: archwudi@zzu.edu.cn

Abstract: As China's "Dual Carbon" strategy is implemented and the new urbanization advances, balancing economic development, emission reduction, and carbon sequestration has become an important issue during the growth of emerging metropolitan areas, and it is also important for achieving high-quality urban development. Therefore, this study had three major objective functions: economic growth, carbon emission reduction, and increased carbon storage. The multi-objective land use quantity structure was solved using the Non-dominated Sorting Genetic Algorithm II (NSGA-II), and the best solution in the solution set was introduced using the Technique for Order Preference by Similarity to Ideal Solution (TOPSIS) for evaluation. Finally, combined with the Future Land Use Simulation (FLUS) model, the low-carbon evolution of the metropolitan area was predicted on a spatial scale. The trade-off plan results show that by 2035, the economic benefits will reach CNY 7.65 trillion, carbon emissions will be kept under 99.24 million tons, and carbon storage will steadily increase by 15.2 million tons. Therefore, optimizing land use from the perspective of balancing carbon emissions, carbon sequestration, and economic development can provide valuable references for planning low-carbon development and the rational use of spatial resources in future metropolitan areas.

Keywords: multi-objective optimization; low-carbon development; multi-model composite; Zhengzhou metropolitan area; China; Land use-cover change

1. Introduction

Since the Industrial Revolution, the continuous advancement of urbanization and the use of fossil fuels to drive large-scale economic growth have led to the massive release of greenhouse gases, primarily carbon emissions, into the environment, exacerbating the global climate crisis [1,2]. To curb global warming and fulfill its commitment to the Paris Agreement, China has pledged to "achieve carbon peak by 2030 and strive for carbon neutrality by 2060". In March 2021, the "14th Five-Year Plan and Long-Range Objectives for National Economic and Social Development of the People's Republic of China and the 2035 Vision Goal Outline" proposed key special tasks to achieve the goals of "carbon peak and carbon neutrality", as well as the new urbanization pattern of "developing and strengthening city clusters and metropolitan areas". As concentrated areas of carbon emissions [3], city clusters and metropolitan areas are also key regions responsible for China's dual carbon strategy [4,5]. In practice, city clusters, as spatial carriers with large scales and high coordination difficulty, present challenges. Metropolitan areas, as an inevitable stage in the development of city clusters and a strategic cornerstone, are undoubtedly the core spatial units for spatial carbon emission reduction and enhancement of carbon sinks [6,7]. Therefore, it is necessary to carry out low-carbon spatial evolution in metropolitan areas and to optimize and upgrade the national territorial spatial pattern.

In recent years, numerous scholars have conducted extensive research on how to reduce carbon in the atmosphere and curb climate change [3,8–10]. Regarding the sources of carbon emissions, from the perspective of the inflow and outflow of carbon elements, carbon sources and carbon sequestration are decisive factors that determine carbon emissions. Carbon sources attributable to human activities can be divided into two aspects: On the one hand, they stem from the consumption of energy sources such as fossil fuels [11], which is closely linked to economic development [12,13]. On the other hand, Land Use and Cover Changes (LUCCs) play a role, where land uses with strong carbon absorption capabilities, such as forests and grasslands, are converted into urban construction land with a negative effect on carbon absorption, releasing carbon sequestered in the soil [14–17]. Carbon sequestration primarily occurs in terrestrial ecosystems [18]. In the field of land use carbon emissions, domestic and international scholars have mainly focused on the effects and influencing factors of carbon emissions [16,19,20], accounting for carbon revenue and expenditure, carbon compensation [21–23], and the carbon trading market [24–26]. Studies, such as those by Chen Jingsong on the Beijing–Tianjin–Hebei region [16] and by Wang Guibo and Chenxu Zhao on Shaanxi Province [27,28], highlight the pivotal role of land conversion in carbon emissions. The establishment of carbon trading markets and the implementation of sensible carbon compensation mechanisms can effectively mitigate regional carbon imbalances arising from global labor division and reduce the costs associated with managing the overall emissions of carbon dioxide [29–32]. Achieving a win-win situation for carbon emission reduction and economic growth has become a consensus among developing countries worldwide [33]. The aforementioned studies elaborated on the relationship between economic growth and carbon emissions, with fewer studies focusing on the path of synergistic promotion of economic growth and reduced carbon emissions [34]. Such synergy only occurs at a low level. Balancing carbon emissions and economic development remains a challenge in current land use optimization [35]. Therefore, the focus of this study was on minimizing carbon emissions and increasing carbon storage while maintaining healthy economic growth.

In current research, land use optimization models are divided into two parts: quantitative structure models and spatial structure models. Quantitative structure prediction models, such as Markov models [36,37], gray models [38], and system dynamics (SD) models [39,40], predict future land use demand based on historical and present land use change trends and their relationships with influencing factors. However, as research progresses, it often encounters multiple objectives that are inherently in conflict, such as food security, ecological service value, and the minimization of carbon emissions [41–44]. These models typically discuss these objectives across various scenarios, and the original quantitative prediction models cannot balance these goals, making it difficult to explore more valuable solutions. Traditional models for handling multi-objective problems, such as the Linear Programming Model (LPM), ideal-point multi-objective linear programming (IMLP), and nonlinear models [45,46], have shown good performance. During the solution process, multiple objectives are assigned weights and transformed into a single objective for resolution. Essentially, this does not optimize multiple objectives to improve land benefits. With the advent of heuristic algorithms that boast enhanced search capabilities and can automatically coordinate multiple objectives without preset weights, genetic algorithms in particular have attracted attention [47–49]. At the same time, NSGA-II has been fully tested and can effectively achieve low-carbon spatial optimization [49,50]. Therefore, for this study, NSGA-II was selected to quantitatively structure the trade-offs of multiple objectives, striving to achieve the optimal land use plan.

Currently, spatial structure models based on Cellular Automata (CA) are dominant, including the CA–Markov model [51–53], CLUE-S models [54,55], PLUS models [56,57], and FLUS models [58–60]. These models each have their characteristics and applications in the simulation of land use and land cover change (LULC) [61]. The CA–Markov model combines the spatial explicitness of Cellular Automata with the probabilistic prediction capabilities of Markov models to forecast regional land use changes and their impacts

on carbon storage [62]. The CLUE-S model utilizes remote sensing data to predict future land use scenarios and assesses the implications of these changes for county-level carbon dioxide emissions [63]. The PLUS model, supported by the Land Expansion Analysis Strategy (LEAS) module, explores the response relationship between urban construction land expansion and carbon emissions at the patch level [64]. The FLUS model is an effective and widely used model for simulating and predicting land use changes and is commonly employed in calculations related to carbon storage [65]. In general, models such as PLUS and CLUE-S predict future spatial patterns based on the transformation rules of various types of land use between two periods of land use data [66]. In contrast, the FLUS model uses single-period data sampling, which reduces error propagation and is more suitable for dealing with the uncertainties and complexities of land use changes [60,66]. Therefore, for this study, the FLUS model was selected to simulate and predict the future spatial optimization evolution of the study area.

This study utilized Python 3.9 to implement the Non-dominated Sorting Genetic Algorithm (NSGA-II), effectively balancing the objectives of maximizing economic benefits, minimizing carbon emissions, and enhancing carbon sequestration. The Pareto optimal solution set was obtained for the future quantitative structure of land use, and the TOPSIS was employed to identify the most balanced solution. Finally, the FLUS model's ANN and CA modules were deployed to simulate the spatial optimization of future land use, aligning economic growth with carbon emissions reduction and carbon storage enhancement. Therefore, this study provides the following insights: (1) The Multi-Objective Optimization Framework integrates these three key objectives into a cohesive strategy, providing innovative insights for land use planning in metropolitan areas and enabling synchronized optimization of multiple goals. (2) This approach enhances the efficiency and precision of selecting optimal solutions from a Pareto front, ensuring a comprehensive strategy for land use planning and revealing the best trade-offs among various objectives.

2. Materials and Methods

2.1. Study Area

The Zhengzhou Metropolitan Area is located at the center of Henan Province, in the middle of China. This area, which is the focus of this study, includes nine cities (Zhengzhou, Kaifeng, Luoyang, Xuchang, Pingdingshan, Luohe, Jiaozuo, Xinxiang, and Jiyuan) and covers a total area of approximately 58,800 km^2, which accounts for 35.49% of the province's total land area, as shown in Figure 1a. In March 2021, the Central Plains Urban Agglomeration was explicitly mentioned in the "14th Five-Year Plan and Long-Range Objectives for National Economic and Social Development of the People's Republic of China and 2035 Vision" for growth and development. As the core of the Central Plains Urban Agglomeration, the Zhengzhou Metropolitan Area was approved by the National Development and Reform Commission in October 2023 and officially became a national-level metropolitan area. The spatial relationship between the two is shown in Figure 1b. Xinxiang City was selected in the first batch of national pilot cities for carbon emission peaking, and Jiyuan City is one of the key construction targets of the national low-carbon city pilot project.

Historical experience has shown that the rapid and uncontrolled expansion of urban agglomerations formed in the early stages of urbanization, along with unbalanced land use patterns, has led to many serious "urban diseases", which, in turn, have restricted the development process of metropolitan areas [67,68]. The Zhengzhou Metropolitan Area is currently in a rapid growth phase. With the increase in population and the expansion of the economic scale, this region faces significant pressure in terms of land resource utilization and ecological and environmental protection. At the same time, the development achievements of the Zhengzhou Metropolitan Area are directly related to the rise of the central region of China and the coordinated development of this region. It is necessary to make scientific decisions, optimize the spatial structure within the "circle", build an ecological security barrier, and guide the metropolitan area towards sustainable and high-

quality development. The study area is located at the junction of the Loess Plateau and the Huang-Huai Plain, and the terrain is mainly high in the west and low in the east. It is situated in the warm temperate zone, crossing the subtropical zone in the south, and has a continental monsoon climate characterized by distinct seasons, which is quite suitable for agricultural development. Affected by national macro-strategic positioning, the proportion of arable land in the entire Zhengzhou Metropolitan Area is significantly higher than those of other types of land use, as shown in Figure 1c. Referring to "Land Use Current Classification" (GB/T 21010-2017), based on the research content and the original classification system of the CLCD, data from each period were reclassified to ultimately obtain six first-level land categories (arable land, forest land, grassland, water areas, construction land, and unused land) as the spatial carriers for the research objects.
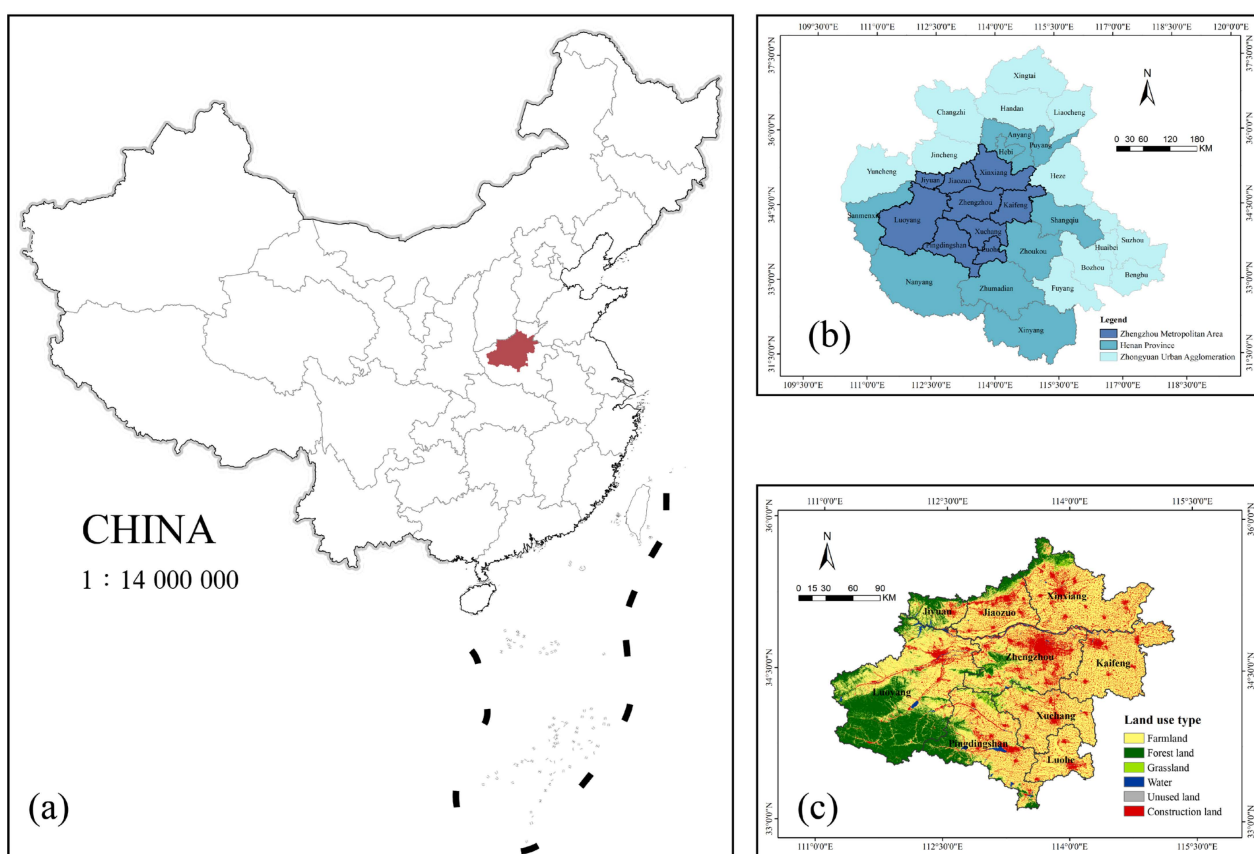

Figure 1. Location of the study area. (**a**) The Zhengzhou Metropolitan Area is located in China. (**b**) The spatial relationship between the Zhengzhou Metropolitan Area, the Central Plains Urban Agglomeration, and Henan Province. (**c**) Land Use Status Classification Map of 2022.

2.2. Data Sources

The data used in this study (Table 1) mainly included elevation data (DEM) sourced from the Geospatial Data Cloud (www.gscloud.cn, accessed on 5 May 2024) that were merged, masked, and extracted in ArcGIS; slope and aspect data derived from the DEM data; annual precipitation data from the ERA5-Land dataset published by the European Union and the European Centre for Medium-Range Weather Forecasts (https://cds.climate.copernicus.eu/, accessed on 4 July 2024); population distribution data from the Oak Ridge National Laboratory (ORNL) of the U.S. Department of Energy; GDP, energy consumption, and other economic and social data from the "Henan Province Statistical Yearbook" and the statistical yearbooks of various cities; and distance data related to water systems, main roads, and railways, all sourced from OpenStreetMap (https://www.openstreetmap.org, accessed on 5 May 2024) and calculated using the Euclidean distance method. This study

utilized land use status data (China Land Cover Dataset, CLCD) from 2015, 2020, and 2022 obtained from a dataset published by [69]. In ArcGIS, land cover data were processed to remove black edges, merged, and clipped. All data were resampled to a resolution of 100 m × 100 m using ArcMap 10.8, and the coordinate system was unified with WGS_1984_UTM_Zone_50N with a grid of 3969 rows × 3357 columns.

Table 1. Data sources.

Data	Sources	Description
Land use type	CLCD Dataset	30 m × 30 m tiff
DEM	www.gscloud.cn	90 m × 90 m tiff
Slope	Calculated from DEM data	90 m × 90 m tiff
Aspect	Calculated from DEM data	90 m × 90 m tiff
Average annual precipitation	ERA5-Land Dataset	1 km × 1 km tiff
Population density	https://www.ornl.gov/	100 m × 100 m tiff
GDP	Statistical Yearbook of Henan Province and Statistical Yearbooks of Various Cities	Number
Energy consumption	Statistical Yearbook of Henan Province and Statistical Yearbooks of Various Cities	Number
Distance to river	https://www.openstreetmap.org	Vector
Distance to railway	https://www.openstreetmap.org	Vector
Distance to road	https://www.openstreetmap.org	Vector
NDVI	http://www.nesdc.org.cn	30 m × 30 m tiff
Night light data	https://www.noaa.gov/	500 m × 500 m tiff

2.3. Methods

Carbon emissions from energy consumption and economic benefits were calculated for the years 2015 to 2022 and assigned to the corresponding land use types, as shown in Figure 2.
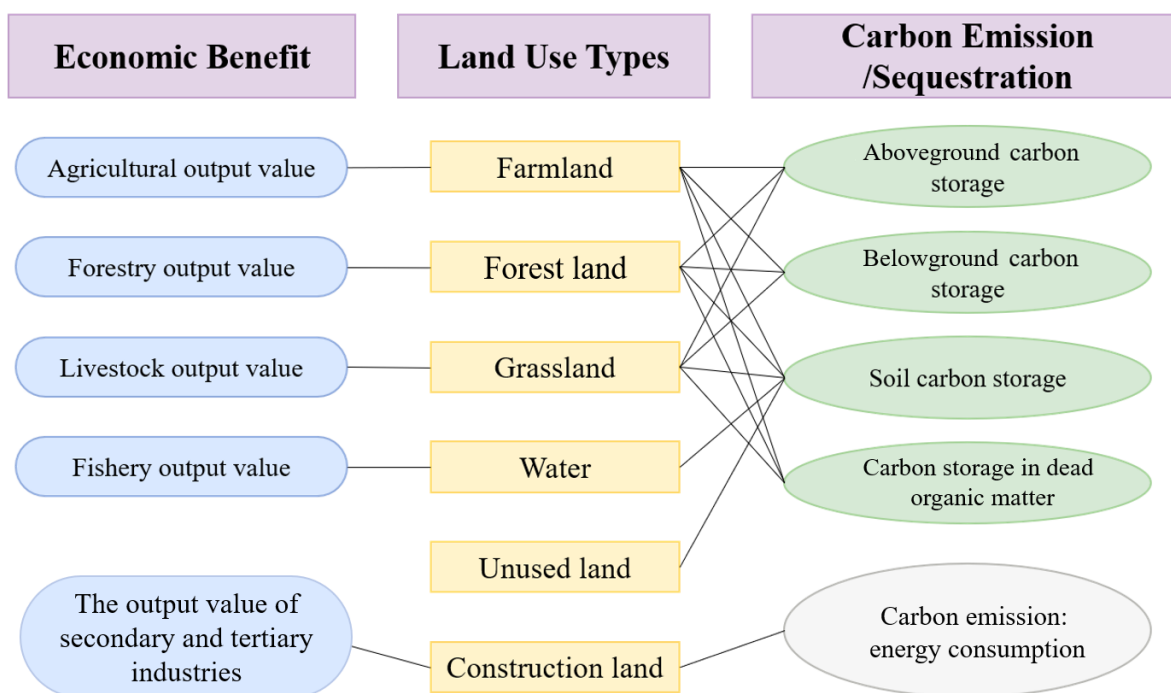

Figure 2. Economic and carbon emission/storage activities assigned to land use types.

In this research, we employed a multi-model approach that incorporated NSGA-II, the TOPSIS, and the FLUS model, and the specific implementation path is illustrated in Figure 3. The gray model was used to predict the growth in energy consumption carbon emissions and economic benefits for the target years. Subsequently, the genetic algorithm NSGA-II was applied to optimize land use allocation with three objectives (maximizing economic benefits, minimizing carbon emissions, and maximizing carbon sequestration), resulting in a series of optimized solution sets. The TOPSIS multicriteria method was utilized to evaluate potential solutions and identified the best solution that balanced these three aspects [48]. Finally, the plans were incorporated into the FLUS model as quantitative units for each type of future land use for spatial optimization, and the specific process is detailed in Figure 3.
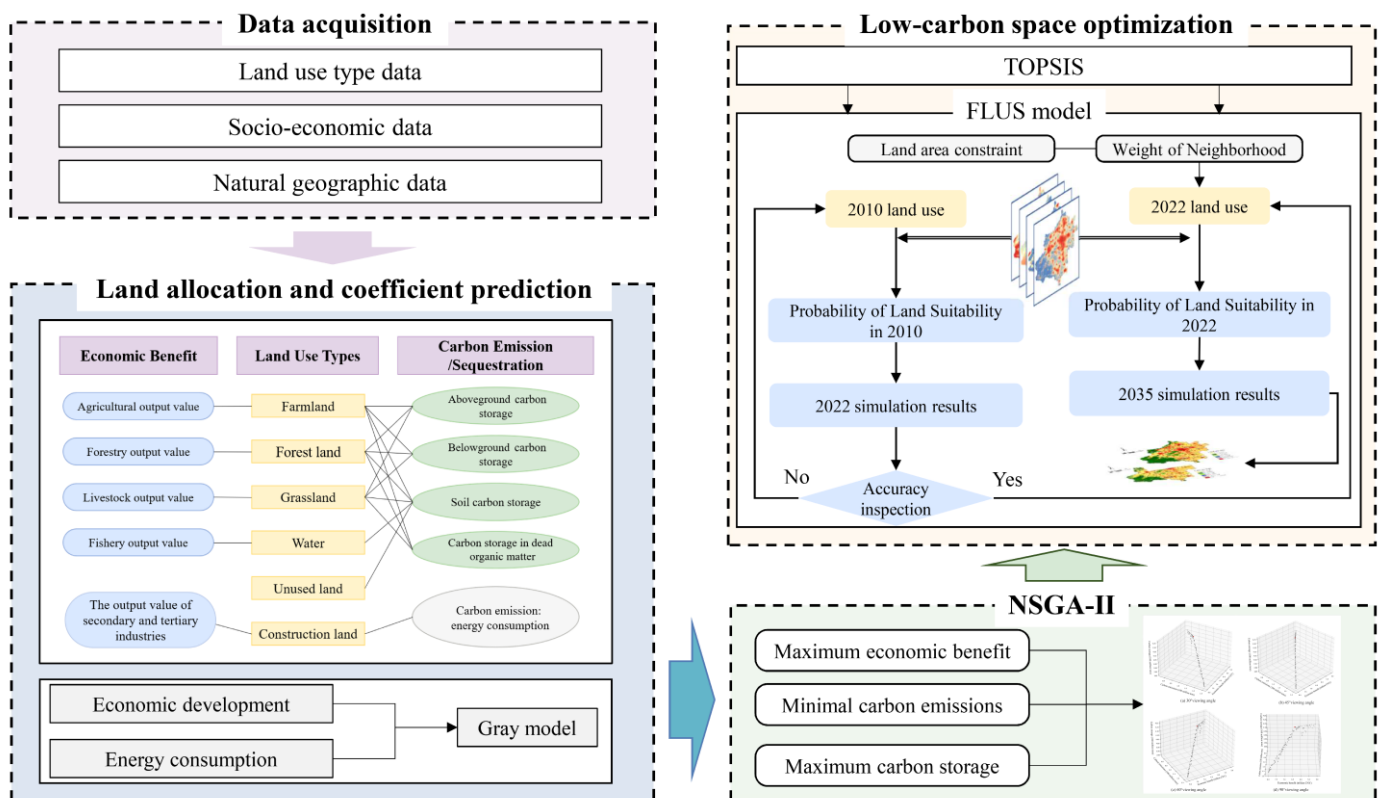

Figure 3. Research framework.

2.3.1. Land Use Allocation and Various Coefficients

- Carbon densities of various land use types

Previous studies have shown that through land management, the carbon storage capacity of soil can be increased, thereby enhancing its potential as a carbon sink [70]. Carbon density data for each land type were derived from four basic carbon pools: aboveground biomass carbon (carbon in all living plant materials above the soil), belowground biomass carbon (carbon present in the living root systems of plants), soil carbon (organic carbon distributed in organic and mineral soils), and dead organic carbon (carbon in litter and dead trees) [71]. The carbon sequestration of land use was calculated by multiplying the carbon density of each land type by its corresponding land area according to the following formula:

$$C_{total} = \sum_{n=1}^{6} A_n (C_{an} + C_{bn} + C_{sn} + C_{on}) \tag{1}$$

where C_{total} represents the total carbon sequestration in the study area; A_n is the area of land use type n; and C_{an}, C_{bn}, C_{sn}, and C_{on} denote the carbon densities of the aboveground biomass carbon pool, belowground biomass carbon pool, soil carbon pool, and dead organic

matter carbon pool for land use type *n*, respectively. During carbon storage estimation, this study assumed that the carbon density remained constant [72,73] and, at the same time, that the carbon density of highly urbanized land can generally be neglected [73]. The average carbon density data for arable land, forest land, grassland, water areas, and unused land in the study area mainly came from previous studies [72,74–77], and the results are shown in Table 2.

Table 2. Carbon densities of various land use types.

Land Use Type	Carbon Density (t/hm^2)
Farmland	66.81
Forest land	149.95
Grassland	72.5
Water	62.1
Construction land	0
Unused land	23.1

Therefore, referring to the land coefficients in Table 2, the objective function for maximizing carbon storage can be constructed as follows:

$$\text{Maximize } F_s = 66.81X_1 + 149.95X_2 + 72.5X_3 + 62.1X_4 + 23.1X_6 \tag{2}$$

where F_s represents the total carbon storage in the study area; X_1 through X_4 represent, in sequence, farmland, forest land, grassland, and water; and X_6 represents unused land.

- Carbon emissions of various land use types

Except for construction land, the coefficient method for calculating carbon emissions was employed for the other five types of land use, with carbon emission coefficients sourced from research findings in Henan Province. The carbon emission coefficients for forest land, grassland, farmland, watersheds, and unused land were −0.61 t/hm^2 [78], −0.021 t/hm^2 [78], 0.422 t/hm^2 [79], −0.253 t/hm^2 [80], and −0.005 t/hm^2 [15]. Carbon emissions from construction land mainly come from human energy consumption, and an indirect estimation method was used based on previous research [73,81]. According to the statistical yearbooks of various cities in Henan Province, which adhere to the "Designated Size Industrial Enterprises", seven types of energy resources required for production and daily living were considered: coal, coke, crude oil, diesel fuel, fuel oil, electricity, and heat. The coefficients used to convert the various fossil fuels to standard coal and their corresponding carbon emission coefficients were referenced from the "China Energy Statistical Yearbook" and the IPCC "Guidelines for National Greenhouse Gas Inventories", as shown in Table 3.

Table 3. Standard coal conversion factors and carbon emission factors.

	Coal	Coke	Crude Oil	Diesel Fuel	Fuel Oil	Electricity	Heat
Conversion coefficient of standard coal	0.7143	0.9714	1.4286	1.4571	1.4286	0.1229	0.0341
Carbon emission coefficient	0.7559	0.8550	0.5857	0.5921	0.6185	0.7935	0.2600

Note: when calculated using standard coal as the unit, the units for coal, coke, crude oil, diesel fuel, and fuel oil are kg per kg of standard coal; the unit for electricity is kg per kWh; and the unit of the carbon emission coefficient, when measured in terms of carbon, is t per t of standard coal.

Based on the calculation of carbon emissions from construction land from 2015 to 2022, the GM(1,1) gray model was used to predict the carbon emission coefficient for the construction land in the study area for the year 2035, which was found to be 79.447 t/hm^2. Therefore, the objective function for minimizing carbon emissions can be constructed as follows:

$$F_c = 0.422X_1 - 0.61X_2 - 0.021X_3 - 0.253X_4 + 79.447X_5 - 0.005X_6 \tag{3}$$

where F_c represents the total carbon emissions in the study area; and X_1 through X_6 represent, in sequence, farmland, forest land, grassland, water, construction land, and unused land.

- Economic benefit coefficients of various land use types

The economic benefit coefficients for the land use types were determined according to the Henan Provincial Statistical Yearbooks from 2015 to 2022, where the economic output of arable land, forest land, grassland, and water areas corresponded to the output values of the agriculture, forestry, animal husbandry, and fishery industries. Construction land was accounted for based on secondary and tertiary industries. Since unused land has virtually no economic activity, its economic benefit coefficient was considered to be 0, as shown in Figure 2. The GM(1,1) gray model was utilized to forecast the economic benefit coefficients for various land use types in the study area for the year 2035 [81], and the results are presented in Table 4.

Table 4. Economic benefit coefficients of various land use types.

	Farmland	Forest Land	Grassland	Water	Construction Land
Economic benefit coefficients (10 thousand/hm²)	12.549	0.722	367.331	22.253	535.853

Therefore, the objective function for maximizing economic benefits can be constructed as follows:

$$F_e = 12.549X_1 + 0.722X_2 + 367.331X_3 + 22.253X_4 + 535.853X_5 \tag{4}$$

where F_e represents the total economic benefit in the study area; and X_1 through X_5 represent, in sequence, farmland, forest land, grassland, water, and construction land.

2.3.2. Multi-Objective Land Use Allocation Method

The multi-objective land use allocation method took into account the requirements of economic development and low-carbon environmental protection, with maximizing economic benefits, minimizing carbon emissions, and maximizing carbon sequestration as the objective functions. This method used six types of land use as decision variables. To ensure that the multi-objective optimization configuration of land use complied with development patterns and policy constraints, several constraints were set in the NSGA-II optimization model. This study used "Henan Province Territorial Spatial Planning (2021–2035)" and other land use planning adjustment texts as its basis and combined the historical land use change situation in the study area to construct constraints for each land type. The total land area in the study area remained constant. According to the plan, the arable land retention in 2035 should not be less than 10,955.52 million mu (approximately 730,368.33 hectares). Based on the third national land survey, the arable land in the study area accounted for 31.73% of the total arable land in the province. Through proportional constraints, the arable land in the study area in 2035 should not be less than 2,317,457.66 hectares. The scale of urban construction land was kept within 1.3 times its scale in 2020. Forest land, grassland, and water areas were set based on previous research [82] and historical land changes. Unused land was set to be non-negative. The framework of the algorithm is shown in Figure 4. The initialization population size was set to 100, the maximum number of iterations was 10,000, the intersection rate was 0.9, and the variation rate was 0.1. Refer to Supplementary Materials for specific code details.
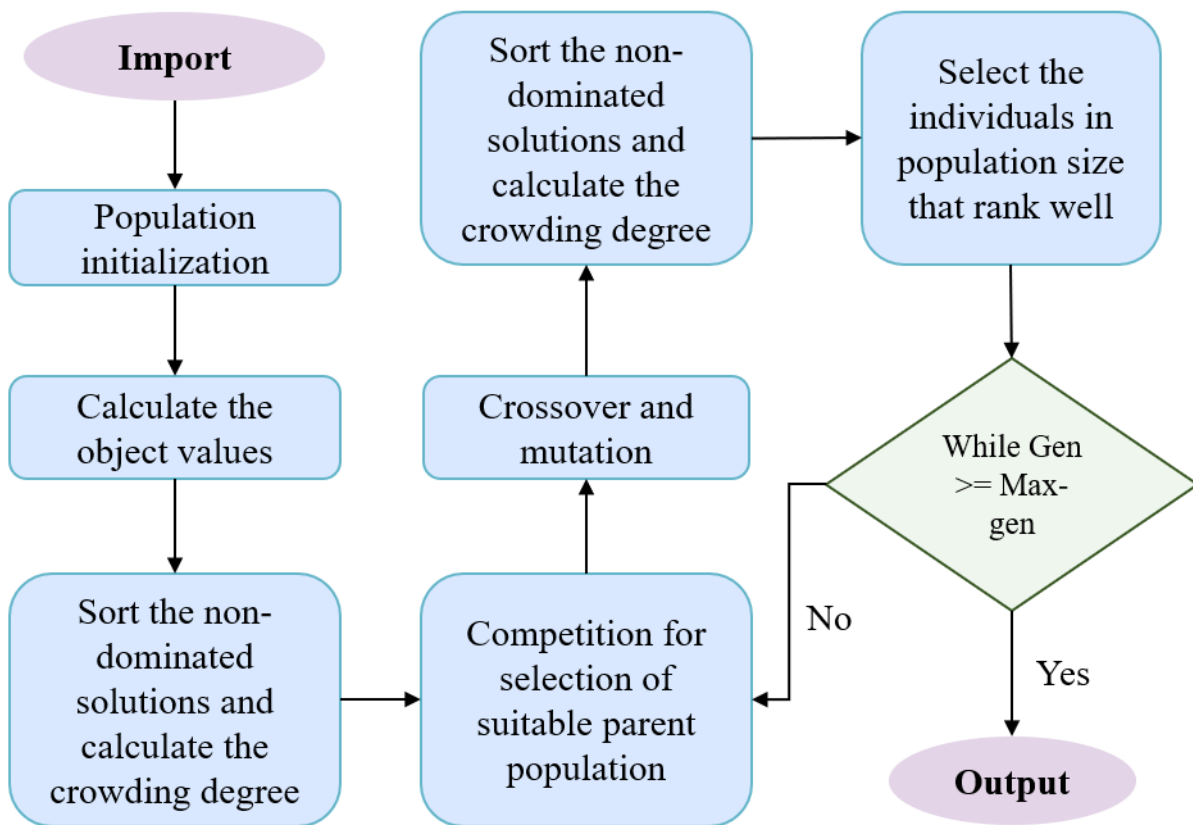
Figure 4. NSGA-II process diagram.

The TOPSIS multicriteria method evaluates the superiority or inferiority of alternative solutions by calculating the distances of each data point from both the positive and negative ideal solutions, followed by a ranking process. Initially, the target values were normalized with the carbon emission targets inverted to ensure that all three objectives were maximized, indicating better performance. The data were then subjected to normalization, and equal weights were assigned to the three objectives. Ultimately, closeness values were derived, and these values were sorted to determine the most and least favorable solutions. For detailed computational formulas, please refer to [48].

2.3.3. Future Land Use Simulation Model

Application of this model began with the use of the Artificial Neural Network (ANN) module to obtain a set of suitability probability maps. This process utilized current land use data and, integrating previous research findings, selected 11 driving factors based on natural and socio-economic conditions, such as elevation, rainfall, population density, and the distance to railways. These factors were normalized, as shown in Figure 5.

This study employed a random sampling strategy with the sampling parameter set to 20 and the number of hidden layers in the neural network set to 13. Based on the historical context change method [81,83], the neighborhood factor and transition cost matrix were configured. The closer the neighborhood factor was to 1, the more easily a land cover type could transform (Table 5). In the cost matrix, 0 indicated that no transformation could occur, while 1 indicated that transformation was possible. Finally, the Kappa index was used to test whether the model's predictions were consistent with the actual results. This index has a range of 0 to 1, and it is generally accepted that a value greater than 0.70 indicates that a model has a high degree of credibility [58,73]. The Kappa index for a land use simulation using the pre-study data from 2010 to 2022 was 0.821877, which was greater than 0.70. Therefore, the FLUS model used in this study was applicable and had a good simulation effect.
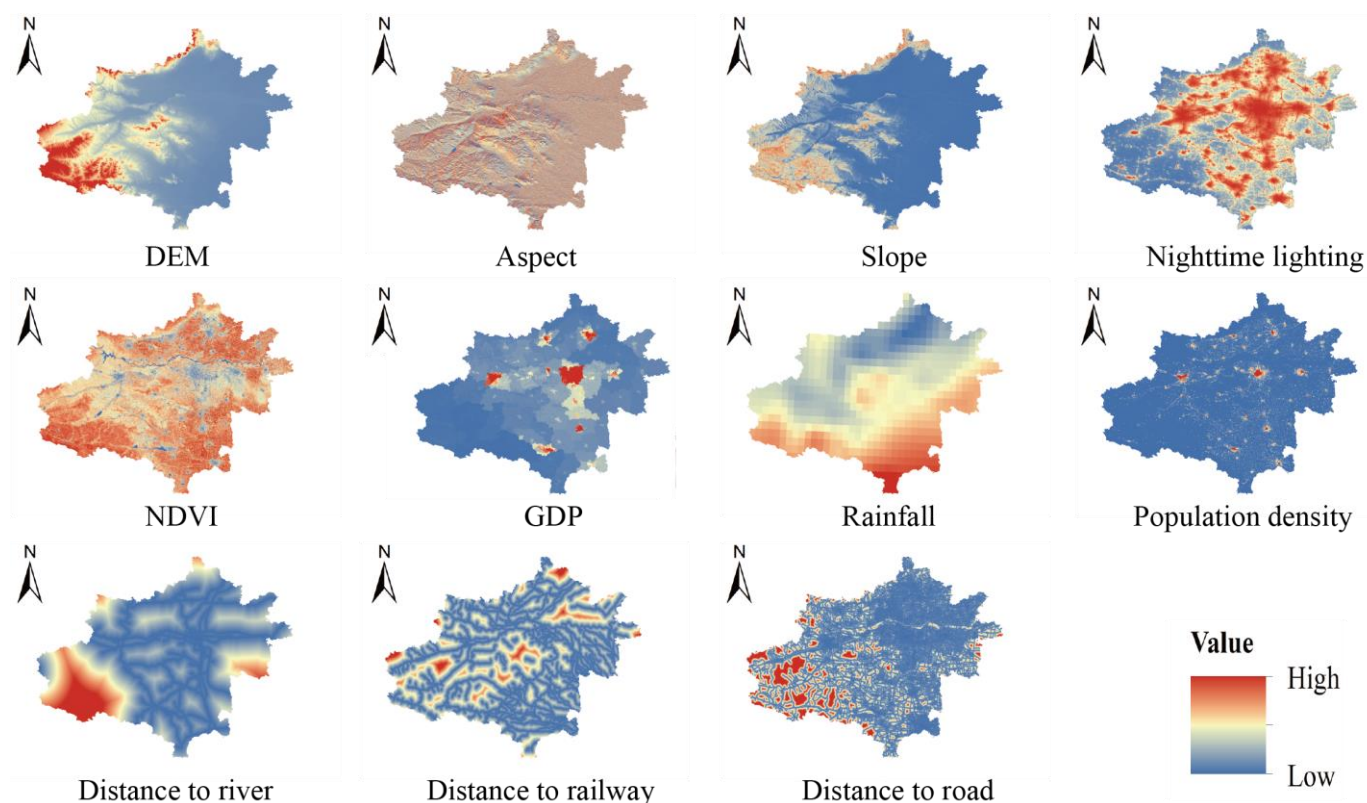
Figure 5. Driving factors in 2022.

Table 5. Neighborhood weight parameters for different land use types.

Land Use Types	Farmland	Forest Land	Grassland	Water	Construction Land	Unused Land
Weight of Neighborhood	0.52901	0.6567	0.0496	0.59267	1	0

3. Results

3.1. The Land Use Changes in the Zhengzhou Metropolitan Area

The Zhengzhou Metropolitan Area experienced land use changes from 2010 to 2022, as depicted in Figure 6. During this period, the areas of both construction land and forest land increased. Construction land expanded by 236,251 hectares, a 28.5% increase, which was the highest among all land use categories. Forest land also increased by 36,178 hectares, a rise of 3.6%. In contrast, arable land, grassland, water bodies, and unused land all experienced decreases. Arable land saw the most significant reduction, with a decrease of 220,219 hectares, accounting for 80.8% of the total decrease and a 5.7% reduction in its proportion. The grassland area shrank by 51,393 hectares, representing 18.8% of the total decrease and a 44.2% reduction in this category. Water bodies decreased by 731 hectares, a 1.1% reduction, and unused land decreased by 86 hectares, a 40.5% reduction.

Over the 12-year period, construction land, forest land, grassland, and water bodies were primarily converted from arable land. Construction land had the most conversions, totaling 85,730 hectares, followed by forest land with 60,248 hectares, grassland with 41,960 hectares, and water bodies with 13,160 hectares. These conversions were also the main reasons for the reductions in grassland and water bodies. Agricultural land and unused land were mainly converted into construction land, with 318,546 hectares and 98 hectares converted, respectively. The conversion of agricultural land was the primary cause of the increase in construction land.
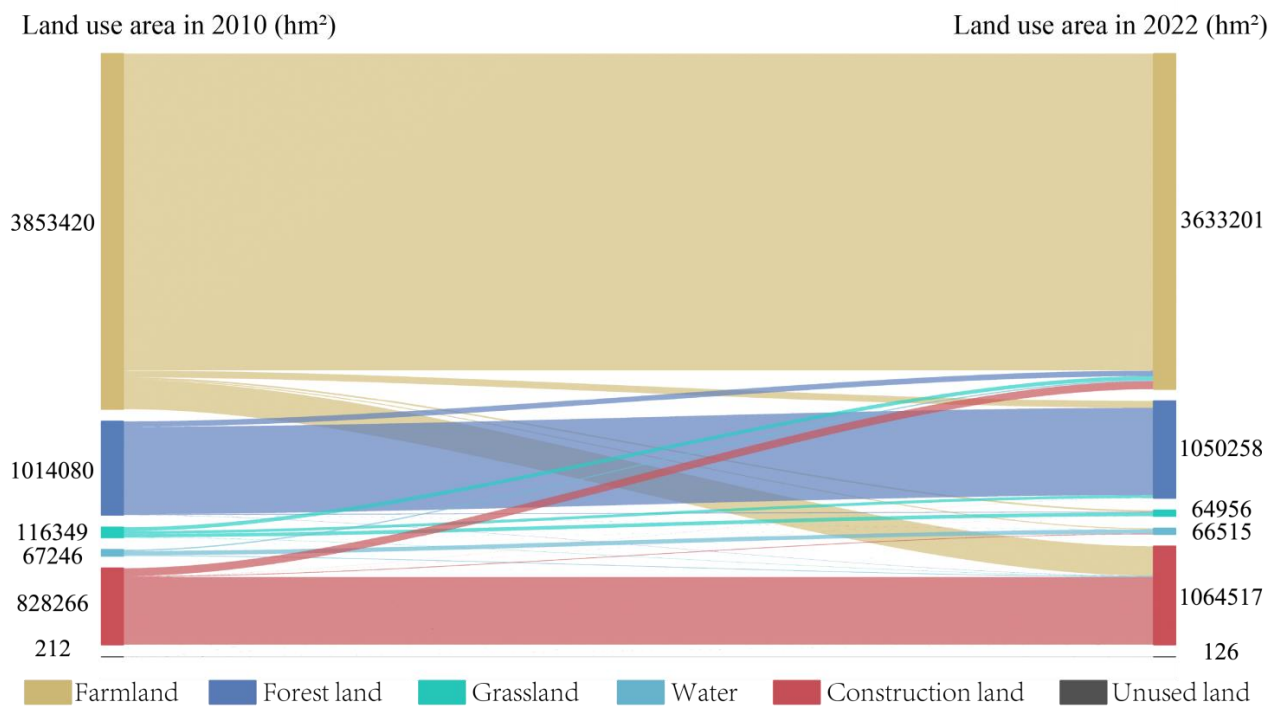
Figure 6. Sankey map of land cover transfer in study area from 2010 to 2022.

3.2. Multi-Objective Pareto Set and TOPSIS Filtering

This study utilized Python 3.9 to invoke NSGA-II from the Geatpy library and implement a multi-objective land use structure optimization plan for the study area in 2035. Ultimately, 100 solutions were retained, which are represented by gray dots in Figure 7. The *X*-axis represents economic benefits in trillions of CNY, the *Y*-axis represents carbon emissions in hundreds of millions of tons, and the *Z*-axis indicates carbon storage in hundreds of millions of tons. After calculation, we first determined three extreme plans for each objective: maximizing economic benefits, minimizing carbon emissions, and maximizing carbon storage. Subsequently, the TOPSIS was used to calculate the closeness to the ideal solution for the three objectives of economic benefits, carbon emissions, and carbon storage in the Pareto set. The closeness results ranged from 0.41 to 0.64, and the value closest to the positive ideal solution was selected. It is marked in red in Figure 6. Observed from multiple perspectives, the red dot is precisely at the turning point of the solution set, indicating that the TOPSIS assessment was better able to select the balance point in the set. The plan could effectively accommodate economic benefits, carbon emissions, and carbon storage.

The results of the multi-objective functions for the four scenarios were compared with the situation in 2022, as shown in Table 6. Looking at the balanced plan, the total annual economic benefit was CNY 7.646 trillion, the carbon emissions were 99.236 million tons, and the land carbon storage was 424.257 million tons. According to Henan Province's "14th Five-Year Plan" and the 2035 vision target, the GDP growth rate should be maintained at around 6%, and by 2035, the total economic benefit will reach about CNY 7.99 trillion. The balanced plan maintained an average annual GDP growth rate of 5.6–5.7%, and this similar growth rate led to a similar result. When maximizing the economic benefits, the overall annual output of the study area was CNY 9.664 trillion, the total carbon emissions were 130.249 million tons, and the carbon storage was 409.06 million tons. When minimizing the carbon emissions, the total annual economic output was CNY 5.994 trillion, the total carbon emissions were 76.09 million tons, and the carbon storage was 416.705 million tons. At the same time, compared with the scenario that maximized the economic benefits, in the balanced plan the total carbon emissions were reduced by a quarter and the carbon storage increased by 10%, adding 3.8165 million tons. Compared with the carbon emission mini-

mization scenario, in the balanced plan both the economic benefits and carbon emissions increased by about 30%.
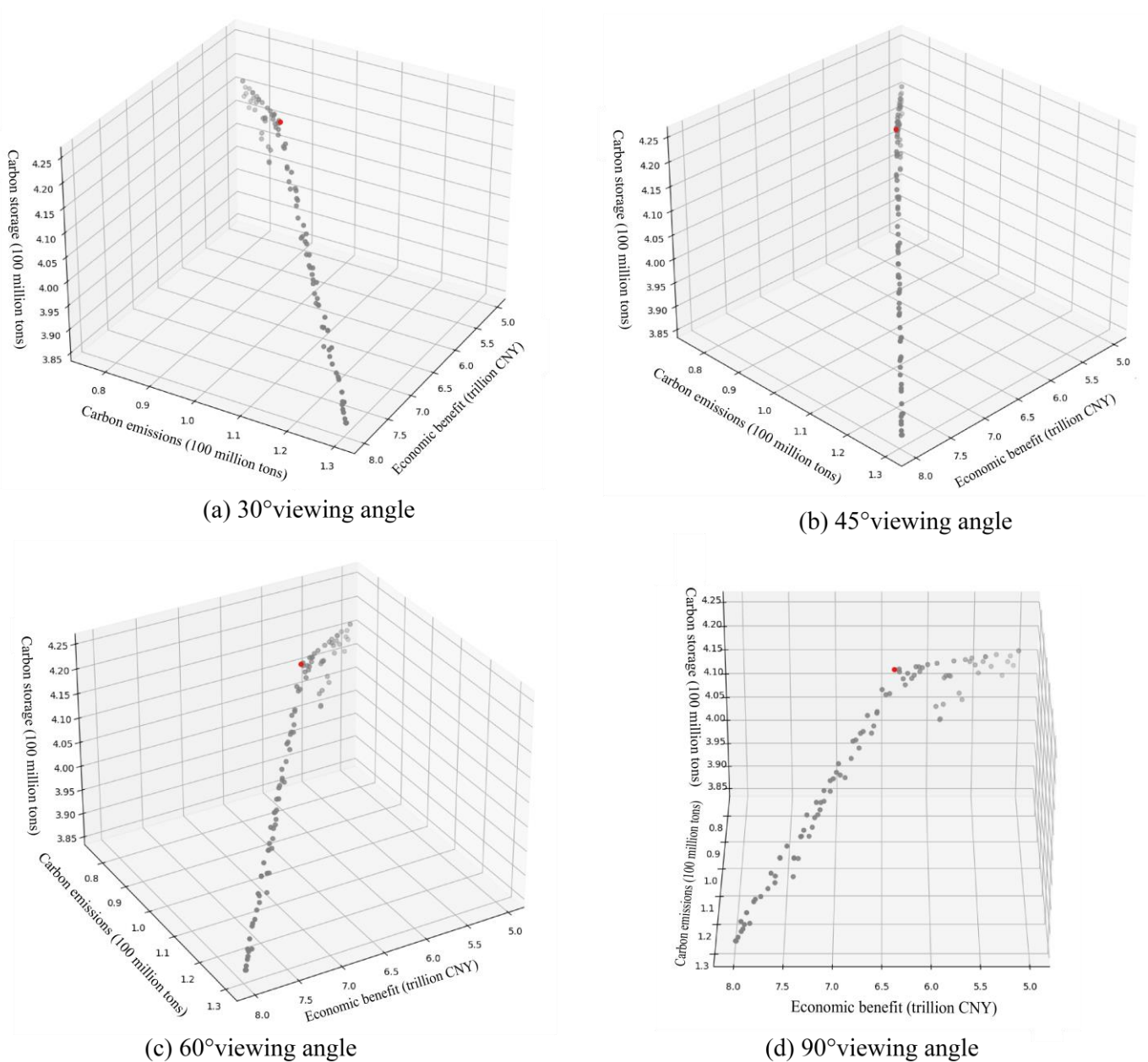

(a) 30°viewing angle

(b) 45°viewing angle

(c) 60°viewing angle

(d) 90°viewing angle

Figure 7. Distribution of Pareto non-dominant solution set for multi-objective functions. (**a–d**) the gray points denote the Pareto solution set, and the red points indicate the selection results.

Table 6. Summary of the results for the three objectives in the different scenarios in 2035.

Results	Economic Benefit (Trillion CNY)	Carbon Emissions (Million Tons)	Carbon Storage (Million Tons)
2022	3.75	68.7	409.06
Maximum economic benefit	9.664	130.249	386.092
Minimum carbon emissions	5.994	76.09	416.705
Maximum carbon storage	7.646	99.236	424.257
Balanced plan	7.646	99.236	424.257

The balanced plan's land quantity structure results were input into the FLUS model, as shown in Figure 8. Panel (a) represents the land use status in 2022, while panel (b) illustrates the balanced optimization outcomes. It is observable that urban construction land is expected to increase significantly, with expansion radiating outwards from the city centers of various urban areas. The central region is anticipated to experience economic growth; however, this is likely to come with a reduction in carbon storage, making it a primary area for potential future increases in carbon emissions. In contrast, continuous reductions in arable land between forest lands in the southwest and northwest—leading to the formation of contiguous forest areas—are expected to be the main source of carbon emission reductions and increases in carbon storage. The emergence of this phenomenon is likely associated with environmental protection measures such as the "Zhengzhou Metropolitan Circle Ecological Protection and Construction Plan (2020–2035)", which has strengthened the forest barriers of the Taihang Mountains in the northwest, Songshan in the central region, and the Funiu Mountains in the southwest of the metropolitan circle. These measures have fortified the ecological defense line, contributing to conservation and enhancing the carbon sequestration capacity in this region.
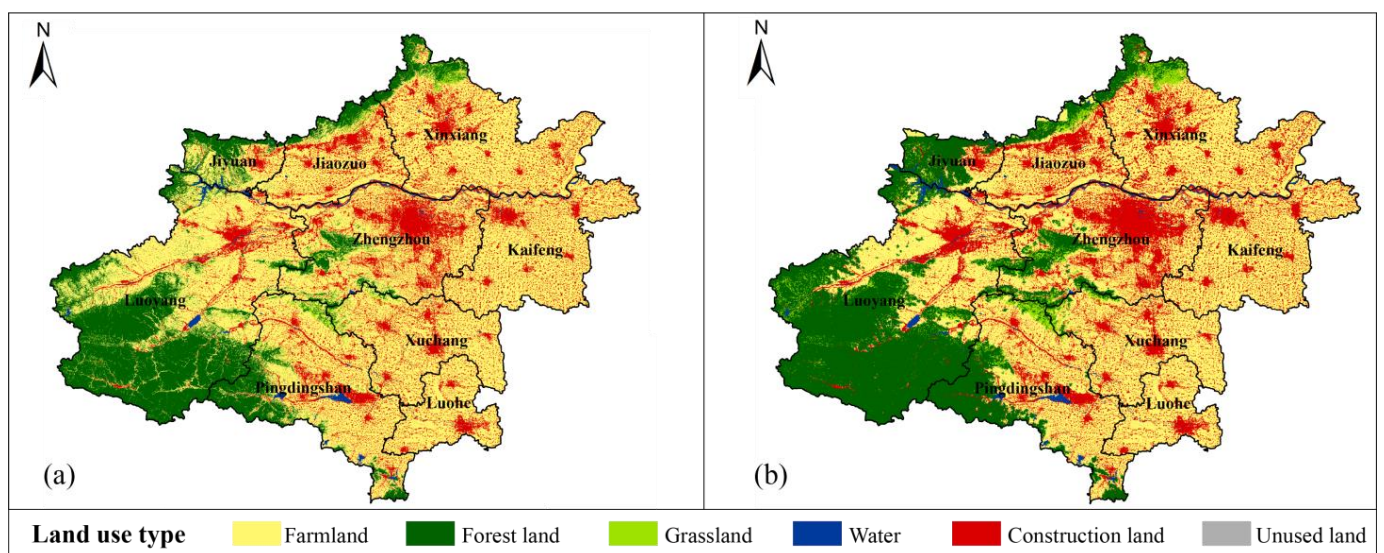

Figure 8. Land use optimization distribution map of Zhengzhou Metropolitan Area in 2035. (**a**) Land Use Status Classification Map of 2022; (**b**) Land Use Simulation Map for 2035.

4. Discussion

4.1. Multi-Objective Low-Carbon Space Optimization

Against the backdrop of the dual carbon goals and new urbanization, achieving low-carbon spatial evolution in metropolitan areas is an inevitable regional mission. However, the development of urban agglomerations is a dynamic and ongoing process, and global research indicates that land use changes exhibit significant regional differences. Studies on land use allocation suggest a gradual shift from singular to composite models [48]. Therefore, this study integrated NSGA-II, the FLUS model, and TOPSIS evaluation to construct a framework for optimizing land use configuration models. It effectively connects land quantitative optimization with spatial structure optimization, providing valuable references for effective land use management in emerging metropolitan areas. On the one hand, considering the multifunctional ability of land to meet the diverse development needs of urban agglomerations, this study addressed the allocation of economic benefits and land types. Li Shaoshuai and colleagues used a genetic algorithm for multi-scenario land optimization, allocating industrial output value only to construction land [82]. Considering that the main activities of tertiary industry also take place on construction land, the economic benefits of construction land included both secondary and tertiary industries in this paper. Moreover,

the corresponding coefficients for energy consumption and economic development in 2035 were predicted using the relatively reliable gray model [42]. Many scholars with different perspectives have used different settings and balances when constructing objective functions that require trade-offs. He Haishan and colleagues, based on the carbon densities and carbon emission coefficients of various land use types, constructed land use structure models for two low-carbon scenarios: maximizing carbon sequestration and minimizing carbon emissions [73]. Yifei Yang and colleagues coupled multiple models and introduced urban form indices in an attempt to focus on both economic and carbon emission benefits using dual structural and spatial dimensions [45]. Yang Lu and colleagues, focusing on pastoral areas, carried out simulations of future land use changes with ecological protection and economic development as their starting points [43]. Based on the NSGA-II and TOPSIS evaluations, this study established a multi-objective function with economic benefits as the goal, low carbon emissions as the premise, and carbon sequestration as an indicator. It calculated a Pareto frontier solution set for each type of land and selected the optimal proportions. This approach not only simulated the multifunctional potential of land for ecology, production, and living but also met the development needs of the metropolitan area for low carbon emissions, increased ecological carbon sequestration, and increased economic growth, properly coordinating regional development contradictions. Subsequently, this study employs the TOPSIS assessment method to discern the optimal decision among the available solution set, corroborated by Wei Li's research [48]. By integrating the NSGA-II with TOPSIS, we have successfully balanced the critical trade-offs between GDP growth, carbon emissions, and carbon sequestration. This represents an advancement in the quantitative optimization of land use, offering a robust framework for decision-making in sustainable development.

4.2. Urban Land Use Strategies

Simply achieving low-carbon cities through urban expansion cannot decouple the association between the economy and carbon emissions. Compared with the carbon emission minimization plan, both the economic benefits and carbon emissions in the balanced plan increased by about 30%, indicating that economic growth in the Zhengzhou Metropolitan Area has not decoupled from carbon emissions. Research by Lei H and colleagues also found that although Chengdu and Xi'an have reached the carbon emission reduction targets, their GDPs have not yet been decoupled from their carbon emissions [84]. In Figure 8, it can be seen that the correlation between carbon emissions and economic benefits is likely due to the increase in construction land in the central region. Research by Wang Guibo and others corroborated this view, stating that construction land, as an important carrier of economic activities, is closely related to carbon emissions [28]. Continuous reductions in arable land between forest lands in the southwest and northwest, with contiguous expansion of forest areas, will be the main source of future carbon emission reductions and increases in carbon storage. Similar studies have indicated that the conversion of ecological land to urban construction land is one of the primary sources of carbon emissions [27,67]. Furthermore, in the spatial arrangement of land use, areas with higher proportions of ecological land use tend to have lower carbon emissions and greater carbon sequestration potential [85]. In addition, managing contiguous areas with the same land use type can also bring about a certain degree of carbon reduction through scale effects. Li and others, by establishing an urban metabolism model in Hangzhou City, found that increasing the relative concentration of the urban population and the scale of the urban land resulted in higher energy efficiency [86]. Gerrit Angst and others also believe that proper land management can not only improve economic benefits but also carbon sink potential [70]. Facing the development path of a high-energy-consumption GDP, measures such as carbon emission trading and carbon taxes can not only adjust the energy structure and reduce differences in carbon emissions between cities but can also control the total regional carbon dioxide emissions at a lower cost, thereby achieving multiple benefits for the metropolitan area [31,32,87]. Referring to Figure 8, the future expansion of construction land in the study

area towards river systems such as the Yellow River implies a rigid requirement for "city planning based on water resources". Future policy development can integrate the research of Yang Zhang and Lirong Liu, among others [87], to utilize the energy–water–carbon nexus to help alleviate the issues of water scarcity, the uneven spatiotemporal distribution of energy, and carbon emissions.

5. Conclusions

Against the backdrop of global warming caused by increasing carbon emissions, as China continues to advance its "dual carbon" goals and the strategy of new urbanization, exploring spatial layout patterns for a low-carbon economy is an essential part of the development of high-quality urban agglomerations. This study utilized NSGA-II to maximize economic benefits, minimize carbon emissions, and maximize carbon sequestration, resulting in a series of solution sets. Subsequently, the TOPSIS was used to evaluate the optimal solution location within the Pareto set. Finally, the optimal solution's trade-off plan for the three objectives was incorporated into the FLUS model to optimize the spatial layout. Considering the trade-off between the economy and carbon emissions while simultaneously taking into account the target of land carbon storage, it is possible to control the peaking and stabilization of carbon emissions while increasing the economic output. The balanced plan achieves an economic benefit of CNY 7.646 trillion in 2035, meeting the economic development requirement guided by policy. The carbon emissions are controlled within 99.236 million tons, and carbon storage grows by 15.197 million tons. According to the spatial layout results for 2035, the expansion of construction land at the centers of urban areas and the "return of farmland to forest" between forests ensure that economic development continues while carbon emissions are controlled and the stability of land carbon storage is guaranteed, enhancing the overall spatial efficiency. These results will be significant for emerging metropolitan areas like the study area when formulating low-carbon development plans for the future.

Future research will address the following limitations: First, macroeconomic development is not a simple linear relationship; therefore, while using the gray model to predict the economic coefficients for 2035, further exploration should be conducted based on the constraints of macroeconomic trends. Secondly, carbon emissions from energy consumption are directly and simply linked to the area of construction land. In fact, newly developed low-carbon technologies, as well as scale effects, can reduce carbon emissions by improving energy efficiency. Therefore, mechanisms should be discussed in the future while considering the impacts of technological elements on carbon reductions.

References

1. Ali, N.S.Y.; See, K.F. Revisiting an environmental efficiency analysis of global airlines: A parametric enhanced hyperbolic distance function. *J. Clean. Prod.* **2023**, *394*, 135982. [CrossRef]
2. Xiao, Y.; Ma, D.; Zhang, F.; Zhao, N.; Wang, L.; Guo, Z.; Zhang, J.; An, B.; Xiao, Y. Spatiotemporal differentiation of carbon emission efficiency and influencing factors: From the perspective of 136 countries. *Sci. Total Environ.* **2023**, *879*, 163032. [CrossRef] [PubMed]

3. Chiquetto, J.B.; Leichsenring, A.R.; Santos, G.M.d. Socioeconomic conditions and fossil fuel CO_2 in the Metropolitan Area of Rio de Janeiro. *Urban Clim.* **2022**, *43*, 101176. [CrossRef]

4. Zhang, J.; Hu, H. Innovation in the Development, Planning and Governance of Metropolitan Areas under the New Development Environment. *Econ. Geogr.* **2023**, *43*, 17–25. [CrossRef]

5. Fang, C. China's Urban Agglomeration and Metropolitan Area Construction Under the New Development Pattern. *Econ. Geogr.* **2021**, *41*, 1–7. [CrossRef]

6. Ma, X.; Chen, Y.; Chen, C.; Xiong, L. Identification and Transformation of the Concepts of Metropolitan Area, Metropolis Area, and Urban Agglomeration. *Planners* **2020**, *36*, 5–11.

7. Long, M.; Li, W.; Hu, M.; Ouyang, P.; Lu, Q. Metropolitan Area Governance and Future Reform in China. *Planners* **2020**, *36*, 12–16.

8. Wang, X.; Lu, F.; Qin, Y.; Sun, Y. Spatial and temporal changes of carbon sources and sinks in Henan Province. *Prog. Geogr.* **2016**, *35*, 941–951. [CrossRef]

9. Zhao, R.; Huang, X.; Chuai, X. Misunderstandings and Future Trends of Researches on Land Use Carbon Emissions in China. *China Land Sci.* **2016**, *30*, 83–92.

10. Hubau, W.; Lewis, S.L.; Phillips, O.L.; Affum-Baffoe, K.; Beeckman, H.; Cuní-Sanchez, A.; Daniels, A.K.; Ewango, C.E.N.; Fauset, S.; Mukinzi, J.M.; et al. Asynchronous carbon sink saturation in African and Amazonian tropical forests. *Nature* **2020**, *579*, 80–87. [CrossRef]

11. IPCC. *2019 Refinement to the 2006 IPCC Guidelines for National Greenhouse Gas Inventory*; IPCC: Geneva, Switzerland, 2019.

12. Dong, Z.; Xia, C.; Fang, K.; Zhang, W. Effect of the carbon emissions trading policy on the co-benefits of carbon emissions reduction and air pollution control. *Energy Policy* **2022**, *165*, 112998. [CrossRef]

13. Wu, Y.; Tam, V.W.Y.; Shuai, C.; Shen, L.; Zhang, Y.; Liao, S. Decoupling China's economic growth from carbon emissions: Empirical studies from 30 Chinese provinces (2001–2015). *Sci. Total Environ.* **2019**, *656*, 576–588. [CrossRef] [PubMed]

14. Deng, W.; Zhu, W.; Zhang, Z.; Li, H.; Hu, J.; Fu, J. Spatio-temporal Variation of Landuse Carbon Budget and Carbon Compensation Zoning at County Level in Henan Province. *Environ. Sci.* **2024**, *49*, 1–24. [CrossRef]

15. Li, L. Research on the Carbon Emission Effect of Land Use in China. Ph.D. Thesis, Nanjing University, Nanjing, China, 2010.

16. Chen, J.; Zhang, J.; Li, J.; Li, S. Spatio-temporal pattern of carbon emissions and its driving factors in the Beijing-Tianjin-Hebei region. *Acta Ecol. Sin.* **2024**, *44*, 2270–2283. [CrossRef]

17. Arneth, A.; Sitch, S.; Pongratz, J.; Stocker, B.D.; Ciais, P.; Poulter, B.; Bayer, A.D.; Bondeau, A.; Calle, L.; Chini, L.P.; et al. Historical carbon dioxide emissions caused by land-use changes are possibly larger than assumed. *Nat. Geosci.* **2017**, *10*, 79–84. [CrossRef]

18. Liu, L.; Song, B. Calculating the carbon sequestration rate of terrestrial ecosystems: Methods, progress and challenges. *Trans. Atmos. Sci.* **2022**, *45*, 321–331. [CrossRef]

19. Fan, J.; Yu, X.; Zhou, L. Carbon emission efficiency growth of land use structure and its spatial correlation: A case study of Nanjing city. *Geogr. Res.* **2018**, *37*, 2177–2192.

20. Wei, W.; Li, Y.; Ma, L.; Xie, B.; Hao, R.; Chen, D.; Yang, S. Carbon emission change based on land use in Gansu Province. *Environ. Monit. Assess.* **2024**, *196*, 311. [CrossRef]

21. Zheng, W.; Kan, Z.; Jie, F. County-level carbon emission accounting and Major Function Oriented Zones in western regions: Taking Sichuan Province as an example. *Acta Ecol. Sin.* **2022**, *42*, 8664–8674.

22. Cai, X.; Ye, C.; Xiao, W.; Peng, J. Spatial Correlation and Carbon Compensation Zoning of Land Use Carbon Budget in the Middle Reaches of Yangtze River. *Resour. Environ. Yangtze Basin* **2024**, *33*, 1474–1488.

23. Xia, M.; Chuai, X.; Xu, H.; Cai, H.H.; Xiang, A.; Lu, J.; Zhang, F.; Li, M. Carbon deficit checks in high resolution and compensation under regional inequity. *J. Environ. Manag.* **2023**, *328*, 116986. [CrossRef] [PubMed]

24. Guo, B.; Feng, Y.; Hu, F. Have carbon emission trading pilot policy improved urban innovation capacity? Evidence from a quasi-natural experiment in China. *Environ. Sci. Pollut. Res.* **2023**, *31*, 10119–10132. [CrossRef] [PubMed]

25. Wang, J.; Wang, B. Employment effect of carbon emission reduction policy: Empirical evidence from carbon trading pilot project. *China Soft Sci.* **2024**, *39*, 156–164.

26. Bian, Z.; Zhong, S. Impact of Carbon Emission Trading Pilot Policy on Urban Land Green Use Efficiency. *China Land Sci.* **2023**, *37*, 52–62. [CrossRef]

27. Zhao, C.; Liu, Y.; Yan, Z. Effects of land-use change on carbon emission and its driving factors in Shaanxi Province from 2000 to 2020. *Environ. Sci. Pollut. Res.* **2023**, *30*, 68313–68326. [CrossRef]

28. Wang, G.; Nan, L. Temporal-Spatial Variance of Carbon Emission Effect in Shaanxi's Land Use. *Resour. Ind.* **2012**, *14*, 124–130. [CrossRef]

29. Chen, H.; Wang, E.; Song, T.; Wang, Y.; Ye, Z. Four-quadrant modelling of carbon inequality in international trade and accounting for carbon compensation. *Carbon Manag.* **2024**, *15*, 2311655. [CrossRef]

30. Zhang, Q.; Jie, D.; Li, J.; Zhou, J. Carbon compensation cost in Jing-Jin-Ji region under the carbon neutrality goal: Considering emission responsibility and carbon abatement cost. *J. Clean. Prod.* **2024**, *467*, 142950. [CrossRef]

31. Liu, Z.; Xu, J. The influence and mechanism of carbon trading pilot on provincial carbon emissions equity: Empirical analysis based on multi-period DID, spatial DID and intermediary effect. *J. Nat. Resour.* **2024**, *39*, 697–711.

32. Yu, X. To promote the stable and sound development of the carbon emissions trading market. *Macroecon. Manag.* **2024**, *40*, 30–37. [CrossRef]

33. Yan, D.; Liu, C.; Li, P. Effect of carbon emissions and the driving mechanism of economic growth target setting: An empirical study of provincial data in China. *J. Clean. Prod.* **2023**, *415*, 137721. [CrossRef]

34. Qin, J.; Ou, D.; Yang, Z.; Gao, X.; Zhong, Y.; Yang, W.; Wu, J.; Yang, Y.; Xia, J.; Liu, Y.; et al. Synergizing economic growth and carbon emission reduction in China: A path to coupling the MFLP and PLUS models for optimizing the territorial spatial functional pattern. *Sci. Total Environ.* **2024**, *929*, 171926. [CrossRef] [PubMed]

35. Hwang, Y.K. The synergy effect through combination of the digital economy and transition to renewable energy on green economic growth: Empirical study of 18 Latin American and caribbean countries. *J. Clean. Prod.* **2023**, *418*, 138146. [CrossRef]

36. Zhu, K.; Cheng, Y.; Zang, W.; Zhou, Q.; El Archi, Y.; Mousazadeh, H.; Kabil, M.; Csobán, K.; Dávid, L.D. Multiscenario Simulation of Land-Use Change in Hubei Province, China Based on the Markov-FLUS Model. *Land* **2023**, *12*, 744. [CrossRef]

37. Mor, B.; Garhwal, S.; Kumar, A. A Systematic Review of Hidden Markov Models and Their Applications. *Arch. Comput. Methods Eng.* **2020**, *28*, 1429–1448. [CrossRef]

38. Yanli, Z.; Yuequn, L.; Heping, L. The Study on Optimization of Land-use Structure Based on Gray Linear Planning in Nanchuan District Chongqing City. *J. Southwest China Norm. Univ. (Nat. Sci. Ed.)* **2009**, *34*, 97–102. [CrossRef]

39. Cao, M.; Chang, L.; Ma, S.; Zhao, Z.; Wu, K.; Hu, X.; Gu, Q.; Lu, G.; Chen, M. Multi-Scenario Simulation of Land Use for Sustainable Development Goals. *IEEE J. Sel. Top. Appl. Earth Obs. Remote Sens.* **2022**, *15*, 2119–2127. [CrossRef]

40. Xing, L.; Xue, M.; Hu, M. Dynamic simulation and assessment of the coupling coordination degree of the economy–resource–environment system: Case of Wuhan City in China. *J. Environ. Manag.* **2019**, *230*, 474–487. [CrossRef]

41. Xin, X.; Zhang, T.; He, F.; Zhang, W.; Chen, K. Assessing and simulating changes in ecosystem service value based on land use/cover change in coastal cities: A case study of Shanghai, China. *Ocean. Coast. Manag.* **2023**, *239*, 106591. [CrossRef]

42. Li, Y.; Liu, X.; Wang, Y.; He, Z. Simulating multiple scenarios of land use/cover change using a coupled model to capture ecological and economic effects. *Land Degrad. Dev.* **2023**, *34*, 2862–2879. [CrossRef]

43. Yang, L.; Xie, Y.; Zong, L.; Qiu, T.; Jiao, J. Land use optimization configuration based on multi- objective genetic algorithm and FLUS model of agro- pastoral ecotone in Northwest China. *J. Geo-Inf. Sci.* **2020**, *22*, 568–579.

44. Wu, X.; Liu, X.; Liang, X.; Chen, G. Multi-scenarios simulation of urban growth boundaries in Pearl River Delta based on FLUS-UGB. *J. Geo-Inf. Sci.* **2018**, *20*, 532–542.

45. Yang, Y.; Xie, B.; Lyu, J.; Liang, X.; Ding, D.; Zhong, Y.; Song, T.; Chen, Q.; Guan, Q. Optimizing urban functional land towards "dual carbon" target: A coupling structural and spatial scales approach. *Cities* **2024**, *148*, 104860. [CrossRef]

46. Li, L.; Huang, X.; Yang, H. Optimizing land use patterns to improve the contribution of land use planning to carbon neutrality target. *Land Use Policy* **2023**, *135*, 106959. [CrossRef]

47. Abdollahi, S.; Ildoromi, A.; Salmanmahini, A.; Fakheran, S. Optimization of geographical space of ecosystem service areas and land-use planning, Iran. *Environ. Monit. Assess.* **2022**, *194*, 527. [CrossRef]

48. Li, W.; Chen, Z.; Li, M.; Zhang, H.; Li, M.; Qiu, X.; Zhou, C. Carbon emission and economic development trade-offs for optimizing land-use allocation in the Yangtze River Delta, China. *Ecol. Indic.* **2023**, *147*, 109950. [CrossRef]

49. Wang, G.; Han, Q.; de Vries, B. The multi-objective spatial optimization of urban land use based on low-carbon city planning. *Ecol. Indic.* **2021**, *125*, 107540. [CrossRef]

50. Liu, H.; Yan, F.; Tian, H. Towards low-carbon cities: Patch-based multi-objective optimization of land use allocation using an improved non-dominated sorting genetic algorithm-II. *Ecol. Indic.* **2022**, *134*, 108455. [CrossRef]

51. Sun, F.; Ge, X.; Jin, M. Temporal and Spatial Variation and Prediction of Land Use and Habitat Quality Based on CA-Markov and InVEST Models in Kunming City. *Areal Res. Dev.* **2024**, *43*, 159–165.

52. Liu, Y.; Li, X.; Yu, X.; Huang, Z. Scenario Simulation of Land Use Change in Chengdu and Carbon Effect Analysis Based on CA-Markov Model. *Sci. Technol. Manag. Land Resour.* **2024**, *41*, 38–49.

53. Yang, J.; Xie, B.; Zhang, D. Spatio-temporal evolution of carbon stocks in the Yellow River Basin based on InVEST and CA-Markov models. *Chin. J. Eco-Agric.* **2021**, *29*, 1018–1029. [CrossRef]

54. Zhu, X.; Guo, Q. Study on scenario simulation of land use spatial pattern based on CLUE-S model—Taking Xinfu District, Xinzhou Cityas an example. *Jiangsu Agric. Sci.* **2020**, *48*, 254–259. [CrossRef]

55. Wei, W.; Xie, Y.; Wei, X.; Xie, B.; Zhang, Q.; Hao, Y. Land Use Optimization Based on CLUE-S Model and Ecological Security Scenario in Shiyang River Basin. *Geomat. Inf. Sci. Wuhan Univ.* **2017**, *42*, 1306–1315. [CrossRef]

56. Wang, J.; Zhang, Z. Land Use Change and Simulation Analysis in the Northern Margin of the Qaidam Basin Based on Markov-PLUS Model. *J. Northwest For. Univ.* **2022**, *37*, 139–148+179.

57. Liang, X.; Guan, Q.; Clarke, K.C.; Liu, S.; Wang, B.; Yao, Y. Understanding the drivers of sustainable land expansion using a patch-generating land use simulation (PLUS) model: A case study in Wuhan, China. *Comput. Environ. Urban Syst.* **2021**, *85*, 101569. [CrossRef]

58. Xue, L.; Wen, L.; Yu, G. Land Cover Simulation and Carbon Storage Assessment in Daqing City based on FLUS-InVEST Model. *Environ. Sci.* **2024**, *49*, 1–15. [CrossRef]

59. Zhang, Y.; Lin, J.; Huang, Y.; Chen, Z.; Zhu, C.; Yuan, H. Delineation of urban growth boundary based on FLUS model under the perspective of land use evaluation in hilly mountainous areas. *J. Mt. Sci.* **2024**, *21*, 1647–1662. [CrossRef]

60. Qi, B.; Yu, M.; Li, Y. Multi-Scenario Prediction of Land-Use Changes and Ecosystem Service Values in the Lhasa River Basin Based on the FLUS-Markov Model. *Land* **2024**, *13*, 597. [CrossRef]

61. Liu, C.; Li, G.; Wu, Z.; He, Y.; Chen, C.; Long, Y. The promotion of sustainable land use planning for the enhancement of ecosystem service capacity: Based on the FLUS-INVEST-RUSLE-CASA model. *PLoS ONE* **2024**, *19*, e0305400. [CrossRef]

62. Zafar, Z.; Zubair, M.; Zha, Y.; Mehmood, M.S.; Rehman, A.; Fahd, S.; Nadeem, A.A. Predictive modeling of regional carbon storage dynamics in response to land use/land cover changes: An InVEST-based analysis. *Ecol. Inform.* **2024**, *82*, 102701. [CrossRef]

63. Wei, T.; Yang, B.; Wang, G.; Yang, K. County land use carbon emission and scenario prediction in Mianyang Science and Technology City New District, Sichuan Province, China. *Sci. Rep.* **2024**, *14*, 9310. [CrossRef] [PubMed]

64. Tian, Y.; Zhao, X. Simulation of construction land expansion and carbon emission response analysis of Changsha-Zhuzhou-Xiangtan Urban Agglomeration based on Markov-PLUS model. *Acta Ecol. Sin.* **2024**, *44*, 129–142. [CrossRef]

65. Lai, J.; Li, J.; Liu, L. Predicting Soil Erosion Using RUSLE and GeoSOS-FLUS Models: A Case Study in Kunming, China. *Forests* **2024**, *15*, 1039. [CrossRef]

66. Liu, H.-L.; Liu, X. The application of ANN-FLUS model in reconstructing historical cropland distribution changes: A case study of Vietnam from 1885 to 2000. *J. Nat. Resour.* **2024**, *39*, 1473–1492. [CrossRef]

67. Chen, X.; Zhao, R.; Shi, P.; Zhang, L.; Yue, X.; Han, Z.; Wang, J.; Dou, H. Land Use Optimization Embedding in Ecological Suitability in the Embryonic Urban Agglomeration. *Land* **2023**, *12*, 1164. [CrossRef]

68. Fang, C. The basic law of the formation and expansion in urban agglomerations. *J. Geogr. Sci.* **2019**, *29*, 1699–1712. [CrossRef]

69. Yang, J.; Huang, X. The 30 m Annual Land Cover Dataset and Its Dynamics in China from 1990 to 2019. *Earth Syst. Sci. Data* **2021**, *13*, 3907–3925. [CrossRef]

70. Angst, G.; Mueller, K.E.; Castellano, M.J.; Vogel, C.; Wiesmeier, M.; Mueller, C.W. Unlocking complex soil systems as carbon sinks: Multi-pool management as the key. *Nat. Commun.* **2023**, *14*, 2967. [CrossRef]

71. Liu, H.; Pan, Y.; Lin, X.; Yang, X.; Gao, Q. Multi-scenario Land Use Optimization and Carbon Storage Evaluation in Central Plains City Cluster of Henan Province. *J. Northwest For. Univ.* **2024**, *39*, 221–230.

72. Li, X.; Wu, K.; Feng, J.; Wang, Y. Carbon balance from the perspective of supply and demand of carbon sequestration services in Henan Province. *Acta Ecol. Sin.* **2022**, *42*, 9627–9635.

73. He, H.; Zhao, Y.; Wu, J. Simulation of urban landscape pattern under the Influence of Low Carbon: A Case Study of Shenzhen. *Acta Ecol. Sin.* **2021**, *41*, 8352–8363.

74. Zhao, W.; Li, L.; Wang, Y.; Li, Y.; Wang, Y.; Wang, X. Carbon sequestration characteristics and regional differences of typical warm and tropical grasslands in Henan Province, China. *Chin. J. Appl. Ecol.* **2018**, *29*, 1867–1875. [CrossRef]

75. Guo, A.; Wang, D.; Yan, K.; Wang, Y.; Yan, D.; Hu, C. CASA Model in Estimating Main Forest Vegetation Carbon in Henan Province. *J. Northeast. For. Univ.* **2023**, *51*, 80–85. [CrossRef]

76. Li, H. Accurate Estimation of Soil Organic Carbon Storage in Henan Province Based on High-Density Profiles. Master's Thesis, Zhengzhou University, Zhengzhou, China, 2016.

77. Xi, X.; Li, M.; Zhang, X.; Zhang, Y.; Zhang, D.; Zhang, J.; Dou, L.; Yang, Y. Research on soil organic carbon distribution and change trend in middle-east plain and its vicinity in China. *Earth Sci. Front.* **2013**, *20*, 154–165.

78. Fang, J.; Guo, Z.; Piao, S.; Chen, A. Estimation of Land Vegetation Carbon Sequestration in China from 1981 to 2000. *Sci. Sin. (Terrae)* **2007**, *37*, 804–812.

79. Zhang, Y.; Dai, Y.; Chen, Y.; Ke, X. The Study on Spatial Correlation of Recessive Land Use Transformation and Land Use Carbon Emission. *China Land Sci.* **2022**, *36*, 100–112.

80. Peng, W.; Zhou, J.; Xu, X.; Peng, H.; Zhao, J.; Yang, C. Effect of land use changes on the temporal and spatial patterns of carbon emissions and carbon footprints in the Sichuan Province of Western China, from 1990 to 2010. *Acta Ecol. Sin.* **2016**, *36*, 7244–7259.

81. Tayier, K.; Li, H.; Aierken, G.; Yin, Z.; Wu, H. Spatio-temporal Evolution and Prediction of Carbon Emissions in Urumqi Region Based on FLUS and Grey Prediction Model. *J. Soil Water Conserv.* **2023**, *37*, 214–226. [CrossRef]

82. Li, S.; Liu, X.; Zhang, C.; Jin, J.; Cao, W.; Lu, J.; Zhang, Y. Multi-objective collaborative optimization allocation of land use in ecologically fragile agricultural areas by coupling NSGA-III and FLUS model. *J. Shaanxi Norm. Univ. (Nat. Sci. Ed.)* **2024**, *52*, 1–11. [CrossRef]

83. Wang, B.; Liao, J.; Zhu, W.; Qiu, Q.; Wang, L.; Tang, L. The weight of neighborhood setting of the FLUS model based on a historical scenario: A case study of land use simulation of urban agglomeration of the Golden Triangle of Southern Fujian in 2030. *Acta Ecol. Sin.* **2019**, *39*, 4284–4298.

84. Lei, H.; Koch, J.; Shi, H.; Zhao, D. Is urban spatial expansion on track to achieve low-carbon cities? An empirical comparative study of Xi'an and Chengdu in western China. *Ecol. Indic.* **2024**, *160*, 111787. [CrossRef]

85. Xia, C.; Chen, B. Urban land-carbon nexus based on ecological network analysis. *Appl. Energy* **2020**, *276*, 115465. [CrossRef]

86. Li, Y.; Shen, J.; Xia, C.; Xiang, M.; Cao, Y.; Yang, J. The impact of urban scale on carbon metabolism -- a case study of Hangzhou, China. *J. Clean. Prod.* **2021**, *292*, 126055. [CrossRef]

87. Zhang, J.; Chen, L.; Xie, Y.; Yang, P.; Li, Z.; Guo, H.; Zhang, Y.; Liu, L. Climate change mitigation in energy-dependent regions—A carbon tax-based cross-system bi-layer model with equilibrium-optimization superposition effects. *Resour. Conserv. Recycl.* **2024**, *200*, 107315. [CrossRef]